MODELLING, CONTROL AND SIMULATION OF PIEZOELECTRIC SMART STRUCTURES USING FINITE ELEMENT METHOD AND OPTIMAL LQ CONTROL

UDC 62-52:62-50:534:531

Ulrich Gabbert[1], Tamara Nestorović Trajkov[1,2], Heinz Köppe[1]

[1]Otto-von-Guericke-Universität Magdeburg, Fakultät für Maschinenbau,
Institut für Mechanik, Universitätsplatz 2, 39106 Magdeburg, Germany
[2]Faculty of Mechanical Engineering, Beogradska 14, 18000 Niš, Yugoslavia

Abstract. *The paper presents some recent developments in modelling and numerical analysis of piezoelectric material systems and controlled smart structures based on a general purpose finite element software with the possibilities of static and dynamic analyses and simulation. Design and simulation of controlled smart structure is also presented, using a state-space model of a structure obtained through the finite element analysis as a starting point for the controller design. For the purpose of the control design for the vibration suppression discrete-time control design tools were used, such as optimal LQ controller incorporated in a tracking system. The application of mentioned methods was verified through the example of actively controlled vibrations of the clamped beam.*

Key words: *piezoelectric smart structures, finite element analysis, optimal LQ control, tracking system.*

1. INTRODUCTION

An increasing interest in the possibilities of active control of structures has given rise to new achievements in this field of research in many branches of engineering over the past few years. In comparison with passive structures, *smart structures* (or *active structures*, or *structronic systems* as they are referred to in different literature) offer a great variety of possibilities for the structural behavior control under changing environment conditions in the sense of adjusting or adapting the structure parameters and behavior to new conditions. From this point of view the term *adaptive structure* is also used to denote the possibility of altering the structural response in the presence of disturbances or changed working conditions. The ability of the structure to change its response in accordance with the changed environment conditions comes from the presence of active materials integrated with the structure. Such active materials (acting as

sensor and/or actuators) in connection with the control system enable automatic adaptation of the structure to changing environment conditions. An important role among active materials belongs to piezoelectric materials (such as thin wafers, fibers or piezoelectric rods) used as actuators and sensors integrated in a structure providing thus the adaptability of the smart structure, while not affecting significantly its passive behavior. Piezoelectric sensing and control with distributed piezoelectric transducers have been intensively studied, e.g. [6], [16], [19]. Application of piezoelectric materials in active structural control requires appropriate simulation and design tools. One of such tools [5] has been developed by the authors (Gabbert *et al.*) and it represents a general purpose finite element based simulation software for piezoelectric smart structures. The software includes an extensive library of coupled finite elements which cover 1D, 2D and 3D continua as well as multilayered composite shell continua based on a general approach. The finite element code includes a substructure technique which provides the possibility of separating mechanical and piezoelectric structures. It also contains a data interface for the communication between finite element analysis tools and controller design tools such as Matlab/Simulink. Theoretical background of the finite element software tool COSAR will be briefly presented in the following chapters.

2. BASIC EQUATIONS OF PIEZOELASTICITY

The coupled electromechanical behavior of a polarizable (but not magnetizable) piezoelectric smart material can be described with adequate accuracy with linearized constitutive equations. These linear equations can be derived from the energy expression [18] in a quadratic form of the primary field variables: mechanical strain $\boldsymbol{\varepsilon}$ and electric field $\mathbf{E}$, on the basis of the assumption that the temperature distribution θ is a priori known or can be calculated independently of the electromechanical fields. The potential function [14], [18] can be written in the following form:

$$H(\boldsymbol{\varepsilon}, \mathbf{E}) = \frac{1}{2}\boldsymbol{\varepsilon}^{\mathrm{T}}\mathbf{C}\boldsymbol{\varepsilon} - \boldsymbol{\varepsilon}^{\mathrm{T}}\mathbf{e}\mathbf{E} - \frac{1}{2}\mathbf{E}^{\mathrm{T}}\boldsymbol{\kappa}\mathbf{E} - \boldsymbol{\varepsilon}^{\mathrm{T}}\boldsymbol{\zeta}\overline{\theta} + \mathbf{E}^{\mathrm{T}}\boldsymbol{\pi}\overline{\theta} . \tag{1}$$

Dependent variables: mechanical stress $\boldsymbol{\sigma}$ and electric displacement $\mathbf{D}$ are derived from (1) by partial differentiation as:

$$\boldsymbol{\sigma} = \frac{\partial H}{\partial \boldsymbol{\varepsilon}} = \mathbf{C}\boldsymbol{\varepsilon} - \mathbf{e}\mathbf{E} - \boldsymbol{\zeta}\overline{\theta}, \quad \mathbf{D} = -\frac{\partial H}{\partial \mathbf{E}} = \mathbf{e}^{\mathrm{T}}\boldsymbol{\varepsilon} + \boldsymbol{\kappa}\mathbf{E} + \boldsymbol{\pi}\overline{\theta}. \tag{2}$$

or in the scalar form [11]:

$$\sigma_{ik} = c_{iklm}^{E}\varepsilon_{lm} - e_{lik}E_l - \lambda_{ik}^{E}\theta, \quad D_i = e_{ilm}\varepsilon_{lm} + \kappa_{il}^{\varepsilon}E_l + p_i^{\varepsilon}\theta. \tag{3}$$

Equations (2) can be written in the matrix notation as:

$$\boldsymbol{\Psi} = \mathbf{J}\boldsymbol{\gamma} - \overline{\boldsymbol{\Theta}} \tag{4}$$

using the following block-matrices:

$$\boldsymbol{\Psi} = \begin{bmatrix} \boldsymbol{\sigma} \\ \mathbf{D} \end{bmatrix}, \quad \mathbf{J} = \begin{bmatrix} \mathbf{C} & \mathbf{e} \\ \mathbf{e}^{\mathrm{T}} & -\boldsymbol{\kappa} \end{bmatrix}, \quad \boldsymbol{\gamma} = \begin{bmatrix} \boldsymbol{\varepsilon} \\ -\mathbf{E} \end{bmatrix}, \quad \overline{\boldsymbol{\Theta}} = \begin{bmatrix} \boldsymbol{\zeta}\overline{\theta} \\ -\boldsymbol{\pi}\overline{\theta} \end{bmatrix} \tag{5}$$

where: $\boldsymbol{\sigma}^T=[\sigma_{11}\ \sigma_{22}\ \sigma_{33}\ \sigma_{12}\ \sigma_{23}\ \sigma_{31}]$ is the stress vector, $\mathbf{C}_{(6\times6)}$ is the symmetric elasticity matrix, $\boldsymbol{\varepsilon}^T=[\varepsilon_{11}\ \varepsilon_{22}\ \varepsilon_{33}\ \varepsilon_{12}\ \varepsilon_{23}\ \varepsilon_{31}]$ is the strain vector, $\mathbf{e}_{(6\times3)}$ is the piezoelectric matrix, $\mathbf{E}^T=[E_1\ E_2\ E_3]$ is the electric field vector, $\boldsymbol{\zeta}$ is the vector of thermal stress coefficients, $\overline{\theta}$ represents the temperature variation of the body with respect to the initial temperature, $\mathbf{D}^T=[D_1\ D_2\ D_3]$ is the vector of electric displacements, $\boldsymbol{\kappa}_{(3\times3)}$ is the symmetric dielectric matrix and $\boldsymbol{\pi}$ is the vector of pyroelectric coefficients.

The linear constitutive equations are an approximation of the real non-linear behavior, which is quite accurate in low electric field applications and gives sufficiently accurate results in most design processes of engineering smart structures.

The constitutive equations (4) together with the mechanical and electric balance equations as well as the mechanical and electric boundary conditions represent a unique set of equations for the coupled electromechanical problem. Equations of motion written in the matrix notation and the charge equation of electrostatics resulting from Maxwell's equations [17] are respectively:

$$\mathbf{L}_u^T\boldsymbol{\sigma} + \overline{\mathbf{p}} - \rho\ddot{\mathbf{u}} = \mathbf{0}, \quad \mathbf{L}_\phi^T\mathbf{D} = \mathbf{0} \qquad \text{in } V \tag{6}$$

where $\overline{\mathbf{p}}^T = \begin{bmatrix}\overline{p}_1 & \overline{p}_2 & \overline{p}_3\end{bmatrix}$ is the body force vector, $\mathbf{u}^T=[u_1\ u_2\ u_3]$ is the vector of mechanical displacements described in Cartesian coordinates system $\boldsymbol{x}^T=[x_1\ x_2\ x_3]$, ρ is the mass density and $\mathbf{L}_u$ and $\mathbf{L}_\phi$ are differentiation matrices:

$$\mathbf{L}_u^T = \begin{bmatrix} \dfrac{\partial}{\partial x_1} & 0 & 0 & \dfrac{\partial}{\partial x_2} & 0 & \dfrac{\partial}{\partial x_3} \\ 0 & \dfrac{\partial}{\partial x_2} & 0 & \dfrac{\partial}{\partial x_1} & \dfrac{\partial}{\partial x_3} & 0 \\ 0 & 0 & \dfrac{\partial}{\partial x_3} & 0 & \dfrac{\partial}{\partial x_2} & \dfrac{\partial}{\partial x_1} \end{bmatrix}, \quad \mathbf{L}_\phi = \begin{bmatrix} \dfrac{\partial}{\partial x_1} \\ \dfrac{\partial}{\partial x_2} \\ \dfrac{\partial}{\partial x_3} \end{bmatrix}. \tag{7}$$

Now the balance equations can be represented in a compact form:

$$\mathbf{L}^T\boldsymbol{\Psi} + \overline{\mathbf{b}} - \rho\ddot{\mathbf{q}} = \mathbf{0} \tag{8}$$

where: $\quad\quad \mathbf{L} = \begin{bmatrix} \mathbf{L}_u & \mathbf{0} \\ \mathbf{0} & \mathbf{L}_\phi \end{bmatrix}, \quad \overline{\mathbf{b}} = \begin{bmatrix} \overline{\mathbf{p}} \\ \mathbf{0} \end{bmatrix}, \quad \rho = \begin{bmatrix} \rho\mathbf{I} & \mathbf{0} \\ \mathbf{0} & \mathbf{0} \end{bmatrix}, \quad \ddot{\mathbf{q}} = \begin{bmatrix} \mathbf{u} \\ \phi \end{bmatrix}. \tag{9}$

The linear strain-displacement relation $\boldsymbol{\varepsilon} = \mathbf{L}_u\mathbf{u}$ and the relation $\mathbf{E} = -\mathbf{L}_\phi\phi$ between the electric field vector $\mathbf{E}$ and electric potential ϕ, can be written together in the form:

$$\boldsymbol{\gamma} = \begin{bmatrix} \boldsymbol{\varepsilon} \\ -\mathbf{E} \end{bmatrix} = \mathbf{Lq}. \tag{10}$$

Taking (10) into account, the constitutive relation (4) can be written in the form:

$$\boldsymbol{\Psi} = \mathbf{JLq} - \overline{\boldsymbol{\Theta}} \tag{11}$$

Now, the balance equation (8) can be written as:

$$\mathbf{L}^T \mathbf{JLq} - \mathbf{L}^T \overline{\mathbf{\Theta}} + \overline{\mathbf{b}} - \rho \ddot{\mathbf{q}} = \mathbf{0} , \tag{12}$$

or in the extended form:

$$\begin{bmatrix} \mathbf{L}_u^T \mathbf{CL}_u & \mathbf{L}_u^T \mathbf{eL}_\phi \\ \mathbf{L}_\phi^T \mathbf{e}^T \mathbf{L}_u & -\mathbf{L}_\phi^T \mathbf{\kappa L}_\phi \end{bmatrix} \begin{bmatrix} \mathbf{u} \\ \phi \end{bmatrix} - \begin{bmatrix} \mathbf{L}_u^T \zeta \overline{\mathbf{\theta}} \\ -\mathbf{L}_\phi^T \pi \overline{\mathbf{\theta}} \end{bmatrix} + \begin{bmatrix} \overline{\mathbf{p}} \\ \mathbf{0} \end{bmatrix} - \begin{bmatrix} \rho \mathbf{I} & \mathbf{0} \\ \mathbf{0} & \mathbf{0} \end{bmatrix} \begin{bmatrix} \ddot{\mathbf{u}} \\ \ddot{\phi} \end{bmatrix} = \mathbf{0} . \tag{13}$$

The mechanical stress and electric charge boundary conditions are:

$$\overline{\mathbf{\tau}} - \mathbf{\tau} = \begin{bmatrix} \overline{\mathbf{t}} \\ \hline \overline{Q} \end{bmatrix} - \mathbf{n\Psi} = \mathbf{0} \qquad \text{on } O_\psi \tag{14}$$

where $\overline{\mathbf{t}}$ is the prescribed traction vector, $\overline{Q}$ is the surface charge, and $\mathbf{n}$ is a matrix of direction cosines which transforms the stresses and electric displacements to the coordinate system normal to the surface. Over bar denotes prescribed values at a particular part of the surface. The boundary conditions of mechanical displacements and electric potential are:

$$\overline{\mathbf{q}} - \mathbf{q} = \mathbf{0} \quad \text{on } O_q. \tag{15}$$

In terms of the weighted residual method, a coupled electromechanical functional is provided by multiplying the balance equation (13) with the vector $\delta \mathbf{q}^T = [\delta \mathbf{u}^T \quad \delta \phi]$ containing the virtual displacement $\delta \mathbf{u}$ and virtual electric potential $\delta \phi$, respectively, and integrating over the entire domain. As a result we obtain:

$$\delta \chi = \int_V \delta \mathbf{q}^T (\mathbf{L}^T \mathbf{JLq} - \mathbf{L}^T \overline{\mathbf{\Theta}} + \overline{\mathbf{b}} - \rho \ddot{\mathbf{u}}) \, dV + \int_{O_t} \delta \mathbf{q}^T (\overline{\mathbf{\tau}} - \mathbf{\tau}) \, dO = \mathbf{0} \tag{16}$$

or in the scalar form [11]:

$$\delta \chi = \int_V \{(\sigma_{ij,j} + \rho \overline{p}_i - \rho \ddot{u}_i) \delta u_i + (D_{i,i}) \delta \phi \} dV + \int_O \{(\overline{q}_i - \sigma_{ij} n_j) \delta u_i - (\overline{Q} + D_i n_i) \delta \phi \} dO = 0 \tag{17}$$

It is assumed that the virtual quantities are admissible, and consequently, fulfill the boundary conditions (15). Using partial integration and the Gaussian integral theorem, the following form of the functional can be derived from (16):

$$\delta \chi = -\int_{V_c} \delta \mathbf{q}^T \rho \ddot{\mathbf{u}} \, dV - \int_{V_c} (\mathbf{L} \delta \mathbf{q})^T \mathbf{JLq} \, dV + \int_{V_c} \delta \mathbf{q}^T \overline{\mathbf{b}} \, dV + \int_{V_c} (\mathbf{L} \delta \mathbf{q})^T \overline{\mathbf{\Theta}} \, dV + \int_{O_t} \delta \mathbf{q}^T \overline{\mathbf{\tau}} \, dO = \mathbf{0} \tag{18}$$

Formulation (18) represents a suitable basis for the development of any type of finite element for coupled electromechanical problems.

3. Finite element analysis of piezomechanical problems

In each finite element the unknown field variables, mechanical displacements u_i and electric potential ϕ are approximated by shape functions $N_k^{(u)}(x)$ and $N_k^{(\phi)}(x)$ in the following way:

$$u_i(x,t) = \sum_{(k)} N_k^{(u)}(x)u_{ik}(t), \quad \phi(x,t) = \sum_{(k)} N_k^{(\phi)}(x)\phi_k(t) \tag{19}$$

where u_{ik} and ϕ_k represent time-dependent unknown nodal values of the element approximate function. In the matrix form these equations can be written as

$$\mathbf{q}(x,t) = \mathbf{N}(x)\mathbf{q}_e(t) \tag{20}$$

where

$$\mathbf{N}(x) = \begin{bmatrix} \mathbf{N}^{(u)} & \mathbf{0} \\ \mathbf{0} & \mathbf{N}^{(\phi)} \end{bmatrix}, \quad \mathbf{q}_e = \begin{bmatrix} \mathbf{u}_e \\ \phi_e \end{bmatrix}. \tag{21}$$

In the previous equation $\mathbf{N}^{(u)}$ and $\mathbf{N}^{(\phi)}$ are the mechanical and electric shape function matrices, respectively, and the vector $\mathbf{q}_e$ contains the mechanical and electric element nodal degrees of freedom $\mathbf{u}_e$ and ϕ_e respectively. Application of the differentiation matrix $\mathbf{L}$ to $\mathbf{q}$ results in

$$\mathbf{Lq} = \mathbf{LNq}_e = \mathbf{Bq}_e \tag{22}$$

where

$$\mathbf{B} = \mathbf{LN} = \begin{bmatrix} \mathbf{L}_u\mathbf{N}^{(u)} & \mathbf{0} \\ \mathbf{0} & \mathbf{L}_\phi\mathbf{N}^{(\phi)} \end{bmatrix}. \tag{23}$$

Introducing the approximate function appearing in (20) into (17) and taking into account (22) as well as $\mathbf{L}\delta\mathbf{q}=\mathbf{LN}\delta\mathbf{q}_e=\mathbf{B}\delta\mathbf{q}_e$ we get:

$$\delta\mathbf{q}_e^{\mathrm{T}}(\mathbf{M}_e\ddot{\mathbf{q}}_e + \mathbf{K}_e\mathbf{q}_e - \mathbf{F}_e) = 0 . \tag{24}$$

If damping is taken into account, the equation of a coupled electromechanical problem in the semi-discrete form becomes:

$$\mathbf{M}_e\ddot{\mathbf{q}}_e + \mathbf{R}_e\dot{\mathbf{q}}_e + \mathbf{K}_e\mathbf{q}_e = \mathbf{F}_e \tag{25}$$

where the mass matrix $\mathbf{M}_e$, generalized stiffness matrix $\mathbf{K}_e$ and generalized force vector $\mathbf{F}_e$ of an element (e) are:

$$\mathbf{M}_e = \int_{V_e}\mathbf{N}^{\mathrm{T}}\boldsymbol{\rho}\mathbf{N}^{\mathrm{T}}dV, \quad \mathbf{K}_e = \int_{V_e}\mathbf{B}^{\mathrm{T}}\mathbf{JB}^{\mathrm{T}}dV, \quad \mathbf{F}_e = \int_{V_e}\mathbf{N}^{\mathrm{T}}\overline{\mathbf{b}}dV + \int_{V_e}\mathbf{B}^{\mathrm{T}}\overline{\boldsymbol{\Theta}}dV + \int_{O_e}\mathbf{N}^{\mathrm{T}}\overline{\boldsymbol{\tau}}dO . \tag{26}$$

4. Placement of actuators and sensors

Placement of actuators and sensors plays an important role in the smart structures design procedure. The effectiveness of the overall smart structure depends to a great extent on the number and distribution of active materials included in a structure as well as

on the designed controller. On the other hand the actuator/sensor locations affect the controllability and the observability of a controlled structure and have a major influence on the efficiency of the control system and the required control effort to satisfy a given design criterion. The placement of actuators/sensors is one of the main problems in the design of adaptive structures. In the distributed control of continua (e.g. plate and shell structures with collocated piezoelectric wafers) the estimation of an optimal actuator and sensor shape as well as their placement are a very complex problem which has not yet been fully solved [11].

In the preliminary steps of the smart structure design it is assumed that the specification of the structure itself, including the objective of the controlled behavior, external disturbances, frequency range etc. is already known. The number and positions of the required actuators and sensors are roughly estimated in the first approach. This can be done on the basis of the controllability and observability indices only, where the influence of the stiffness and the mass changes due to the active materials as well as the controller influence are omitted. Based on the results of an eigenvalue analysis at each structural point the modal strains and consequently the modal electric voltage can be calculated which in principal results in the controllability index $\mu_k(\mathbf{x}_P)$ of the kth mode at the position $\mathbf{x}_P$. The best positions $\mathbf{x}_P$ to control the first r eigenmodes are those positions where the overall controllability index

$$\mu(\mathbf{x}_P) = \prod_{k=1}^{r} w_k \mu_k(\mathbf{x}_P) \tag{27}$$

has the largest value.

5. DEVELOPMENT OF THE STATE-SPACE MODEL AND DATA EXCHANGE

For the purpose of the overall smart structure design and simulation, besides the active sensor/actuator elements, an appropriate model of the controller is required. The procedure of the control law design, testing and verification in the framework of the finite element analysis represents in general a complex process which requires some additional tools to support design process. MATLAB/SIMULINK is a convenient environment for the controller design and simulation with many available tools for this purpose and for that reason it was reasonable to create an interface which would provide data exchange between the finite element analysis code and the controller design tool. In this case this data exchange should be bi-directional since the data from the finite element model such as the mass matrix, the stiffness matrix, the damping matrix as well as sensor and actuator positions are required to design the controller and on the other hand the controller matrix (or subroutines calculating the controller parameters) is needed in the finite element package to simulate the controlled structural behavior [11]. For the exchange of data and information between the finite element package COSAR [5] and MATLAB/SIMULINK, a general data exchange interface has been designed and implemented in the finite element software. The communication concept between the finite element software COSAR and MATLAB/SIMULINK is shown in Fig. 1.
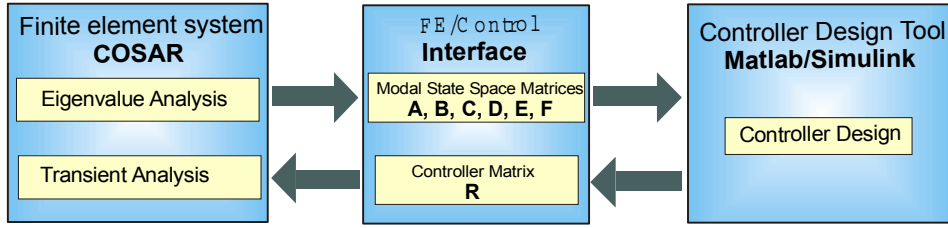
Fig. 1. Data exchange between the finite element software COSAR and MATLAB/SIMULINK

Controller design for a flexible mechanical structure represents in general case a *multiple input - multiple output* (MIMO) problem, where the application of large-scale finite element models is not suitable due to the high order of the resulting state-space model. Therefore, an appropriate model reduction technique is required to reduce the number of the finite element equations. One of the best-known model reduction techniques is the modal truncation. This technique has been combined with the investigations of the dominant behavior of different modes. The modal truncation seems to be best suited for the controller design of structures based on a finite element discretization, since flexible structures possess a low-pass characteristic, which allows neglecting high-frequency dynamics. This technique based on the solution of the linear eigenvalue problem

$$(\mathbf{K} - \lambda_k \mathbf{M})\boldsymbol{\varphi}_k = \mathbf{0} \tag{28}$$

results in the ($n \times r$) modal matrix $\boldsymbol{\Phi} = [\boldsymbol{\varphi}_1 \vdots \boldsymbol{\varphi}_2 \vdots \cdots \vdots \boldsymbol{\varphi}_r]$ and the ($r \times r$) spectral matrix $\boldsymbol{\Lambda} = diag(\lambda_k)$, where $\boldsymbol{\Phi}$ is ortho-normalized with $\boldsymbol{\Phi}^{\mathrm{T}}\mathbf{M}\boldsymbol{\Phi} = \mathbf{I} = diag(1)$ and $\boldsymbol{\Phi}^{\mathrm{T}}\mathbf{K}\boldsymbol{\Phi} = \boldsymbol{\Lambda}$. Consequently, inserting the modal coordinates $\mathbf{q} = \boldsymbol{\Phi}\mathbf{x}$ into (25) results in a truncated system of r differential equations which can be written as

$$\ddot{\mathbf{x}} + \boldsymbol{\Delta}\dot{\mathbf{x}} + \boldsymbol{\Lambda}\mathbf{x} = \boldsymbol{\Phi}^{\mathrm{T}}\overline{\mathbf{E}}\mathbf{f}(t) + \boldsymbol{\Phi}^{\mathrm{T}}\overline{\mathbf{B}}\mathbf{u}(t). \tag{29}$$

Usually, in spite of the system reduction the classical controller design methods in the frequency domain cannot be applied. Therefore, the controller description is given in the state-space form. It is assumed that the equation of motion is reduced to the first r eigenvectors, which results in (29). Defining the state vector as:

$$\mathbf{z} = \begin{bmatrix} \mathbf{x} \\ \dot{\mathbf{x}} \end{bmatrix}, \tag{30}$$

the modal reduced model (29) can be transformed into the modal form of the state-space equation:

$$\dot{\mathbf{z}} = \begin{bmatrix} \mathbf{0} & \mathbf{I} \\ -\boldsymbol{\Lambda} & -\boldsymbol{\Delta} \end{bmatrix}\mathbf{z} + \begin{bmatrix} \mathbf{0} \\ \boldsymbol{\Phi}^{\mathrm{T}}\overline{\mathbf{B}} \end{bmatrix}\mathbf{u}(t) + \begin{bmatrix} \mathbf{0} \\ \boldsymbol{\Phi}^{\mathrm{T}}\overline{\mathbf{E}} \end{bmatrix}\mathbf{f}(t) = \mathbf{A}\mathbf{z} + \mathbf{B}\mathbf{u}(t) + \mathbf{E}\mathbf{f}(t). \tag{31}$$

Together with the modal form of the measurement equation

$$\mathbf{y} = \mathbf{C}\mathbf{z} + \mathbf{D}\mathbf{u}(t) + \mathbf{F}\mathbf{f}(t), \tag{32}$$

which can also be established based on the data of the finite element model, all required information to design an appropriate controller are prepared. The matrices **A**, **B**, **C**, **D**, **E**, **F** are transferred to MATLAB/SIMULINK via the data interface (Fig. 1) to design the controller and to test it through numerical experiments. The controller can also be directly implemented on a dSPACE system, which enables designer to work in a *hardware-in-the-loop* configuration in order to test and modify designed controller on the bases of real experiments. But before performing such experiments the structural behavior can also be tested on a virtual computer model of the structure, which is based on the original finite element model. Therefore the controller can be transformed back into the finite element software via the data interface, where in LTI systems the designed controller matrix **L** is used to generate the actuator signal as

$$\mathbf{u}(t) = -\mathbf{L}\mathbf{y}(t). \tag{33}$$

The controller can also be directly implemented in the finite element software as C-code subroutine resulting from MATLAB/SIMULINK.

6. CONTROLLER DESIGN

The controller design starts with the continuous state-space model:

$$\dot{x} = \mathbf{A}x + \mathbf{B}u + \mathbf{E}d$$
$$y = \mathbf{C}x + \mathbf{D}u + \mathbf{F}d \tag{34}$$

the state matrices of which are obtained through the finite element analysis and modal reduction described previously. The general form of the plant model (34) assumes the presence of disturbance *d* in the state and output equations. Hence, the controller is designed introducing additional dynamics [20] to compensate for the presence of disturbances and to provide tracking of the reference input with prescribed frequency in order to suppress vibrations. Additional dynamics is formed based on the assumption that the reference input to be tracked and disturbance that acts upon the structure can be described by the rational discrete transfer function. Sine function fulfils this condition and it is usually used as a disturbance model.

For discrete-time controller design it is necessary to obtain discrete-time state space model of the plant-structure. It is obtained from (34) by discretization with the appropriate sampling time *T*. Discrete-time model is in the form:

$$x[k+1] = \mathbf{\Phi}x[k] + \mathbf{\Gamma}u[k] + \varepsilon d[k] \qquad y[k] = \mathbf{C}x[k] + \mathbf{D}u[k] + \mathbf{F}d[k] \tag{35}$$

where:
$$\mathbf{\Phi} = e^{\mathbf{A}T}, \quad \mathbf{\Gamma} = \int_0^T e^{\mathbf{A}\tau}\mathbf{B}d\tau, \quad \varepsilon = \int_0^T e^{\mathbf{A}\tau}\mathbf{E}d\tau. \tag{36}$$

Additional dynamics is determined in the state-space form on the basis of disturbance and/or reference input poles λ_i. Based on the coefficients of the polynomial:

$$\delta(z) = \prod_i (z - e^{\lambda_i T})^{m_i} \overset{def}{=} z^s + \delta_1 z^{s-1} + \ldots + \delta_s, \tag{37}$$

obtained by mapping the pole locations into the z-plane, the additional dynamics, described by $\mathbf{\Phi}_a$ and $\mathbf{\Gamma}_a$ matrices:

$$\mathbf{\Phi}_a = \begin{bmatrix} -\delta_1 & 1 & 0 & \cdots & 0 \\ -\delta_2 & 0 & 1 & \cdots & 0 \\ \vdots & \vdots & \vdots & \ddots & \vdots \\ -\delta_{s-1} & 0 & 0 & \cdots & 1 \\ -\delta_s & 0 & 0 & \cdots & 0 \end{bmatrix}, \quad \mathbf{\Gamma}_a = \begin{bmatrix} -\delta_1 \\ -\delta_2 \\ \vdots \\ -\delta_{s-1} \\ -\delta_s \end{bmatrix}, \tag{38}$$

is formed.

Discrete-time design model ($\mathbf{\Phi}_d$, $\mathbf{\Gamma}_d$) is formed as a cascade combination of additional dynamics ($\mathbf{\Phi}_a$, $\mathbf{\Gamma}_a$) and discrete-time plant model ($\mathbf{\Phi}$, $\mathbf{\Gamma}$) obtained for specified sampling time T:

$$x_d[k+1] = \mathbf{\Phi}_d x_d[k] + \mathbf{\Gamma}_d u[k] \tag{39}$$

where:
$$x_d[k] = \begin{bmatrix} x[k] \\ x_a[k] \end{bmatrix}, \quad \mathbf{\Phi}_d = \begin{bmatrix} \mathbf{\Phi} & 0 \\ \mathbf{\Gamma}_a \mathbf{C} & \mathbf{\Phi}_a \end{bmatrix}, \quad \mathbf{\Gamma}_d = \begin{bmatrix} \mathbf{\Gamma} \\ 0 \end{bmatrix}. \tag{40}$$

Feedback gain matrix $\mathbf{L}$ of the optimal LQ regulator is calculated on the basis of design model (39) in such a way that the feedback law $u[k] = -\mathbf{L}x_d[k]$ minimizes the performance index:

$$J = \frac{1}{2} \sum_{k=0}^{\infty} (x_d[k]^T \mathbf{Q} x_d[k] + u[k]^T \mathbf{R} u[k]) \tag{41}$$

subject to the constraint equation (39) where $\mathbf{Q}$ and $\mathbf{R}$ are symmetric, positive-definite matrices. Feedback gain matrix $\mathbf{L}$ is afterwards partitioned into submatrices $\mathbf{L}_1$ and $\mathbf{L}_2$ corresponding to the plant and additional dynamics, respectively. Partitioned feedback gain matrix is implemented in the control system as shown in Fig.2.
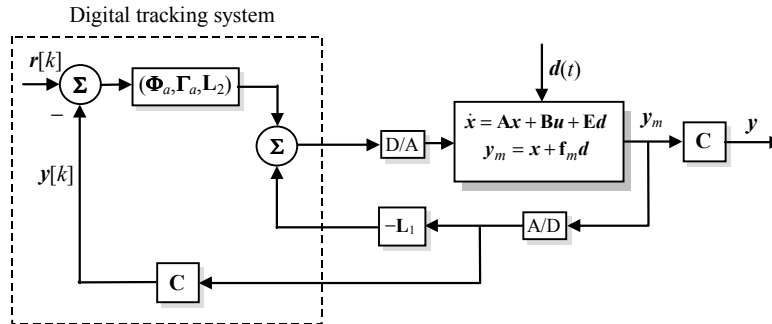

Fig. 2. Optimal LQ tracking system

7. VIBRATION SUPPRESION OF THE ACTIVLY CONTROLLED CLAMPED BEAM

Numerical experiment was performed on the test example of the clamped beam. Applying the procedure described above, optimal LQ tracking system was designed for

the purpose of the clamped beam vibration suppression in the presence of sine-type disturbance forces acting on the corner points of the free beam end (Fig. 3). State space model for the controller design was obtained through the finite element analysis.

Clamped beam shown in Fig. 3 represents active plate structure controlled by four piezoelectric patch actuators attached to the beam, two on the top and two on the bottom of the plate. Geometry of the plant as well as the plate, actuator and sensor properties are listed in Fig. 3. At first step the plant was represented in the form of a finite element model with a mesh of 235 passive and 80 active Semiloof shell elements [2], [7], [8]. On the basis of this mesh the eigenfrequencies and eigenmodes were calculated. Considered frequencies which are of interest for bending mode study cases are f_1=17.2Hz, f_2=108.6Hz, f_4=302.9Hz and f_6=606.1Hz.
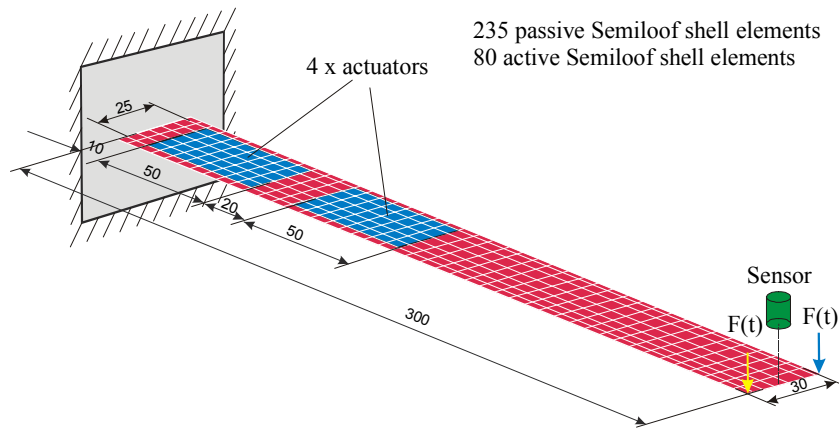
Material:

Beam:
E = 2.00·10^5 N/mm²
ν = 0.3
ρ = 7.86·10^{-9} Ns²/mm⁴

Actuator/sensor:
E_{11} = E_{22}=3.77·10^4 N/mm²
G_{12} = 1.3·10^4 N/mm²
ν = 0.38
t = 2.0 mm (thickness)

d_{31} = 2.1·10^{-7} mm/V
$κ_{33}$ = 3.36·10^{-9} F/m
t = 0.4 mm (thickness)

Fig. 3. Actively controlled clamped beam

Plate model was modally reduced and transformed into the state-space model using the finite element software [5]. Via data exchange interface the model in the form (34) was exported into MATLAB/SIMULINK as a software environment for controller design and testing. Appropriate state-space matrices in the model (34) are:

$$\mathbf{A} = 10^7 \cdot \begin{bmatrix} 0 & 0 & 0 & 0 & 0.0000001 & 0 & 0 & 0 \\ 0 & 0 & 0 & 0 & 0 & -0.046581 & 0 & 0 \\ 0 & 0 & 0 & 0 & 0 & 0 & 0.00000010 & 0 \\ 0 & 0 & 0 & 0 & 0 & 0 & 0 & 0.00000010 \\ -0.001171 & 0 & 0 & 0 & -0.000002 & 0 & 0 & 0 \\ 0 & -0.04658 & 0 & 0 & 0 & -0.000002 & 0 & 0 \\ 0 & 0 & -0.362499 & 0 & 0 & 0 & -0.00000080 & 0 \\ 0 & 0 & 0 & -1.450350 & 0 & 0 & 0 & 0.00000122 \end{bmatrix}$$

$$\mathbf{B} = 10^3 \cdot \begin{bmatrix} 0 & 0 & 0 & 0 \\ 0 & 0 & 0 & 0 \\ 0 & 0 & 0 & 0 \\ 0 & 0 & 0 & 0 \\ -0.00608366 & 0.00608367 & -0.00366187 & 0.00366187 \\ -0.13753931 & 0.13753931 & 0.13713482 & -0.13713482 \\ -0.34219542 & 0.34219542 & 1.21732159 & -1.21732161 \\ -1.08861338 & 1.08861361 & 0.10482408 & -0.10482390 \end{bmatrix}, \quad \mathbf{E} = 10^5 \cdot \begin{bmatrix} 0 & 0 \\ 0 & 0 \\ 0 & 0 \\ 0 & 0 \\ 0.18138856 & 0.18138856 \\ -1.11557656 & -1.11557656 \\ 3.23297778 & 3.23297781 \\ 6.25304539 & 6.25313464 \end{bmatrix},$$

$$\mathbf{C} = [1.54877435 \quad -0.23953924 \quad 0.0893192 \quad 0.04332433 \quad 0 \quad 0 \quad 0 \quad 0], \quad \mathbf{D} = [0 \quad 0 \quad 0 \quad 0], \quad \mathbf{F} = [0 \quad 0].$$

Exciting forces $F(t) = A\sin(\omega_i t) = A\sin(2\pi f_i t)$, $A = 0.01$, exerted at the corner points of the beam end were chosen according to the eigenfrequencies of interest, considering such disturbance as the worst case due to the possibility of the resonance. Since disturbance is a sine function, its s-plane poles are complex conjugate numbers $\lambda_{1,2} = \pm j\omega_i$, where $\omega_i = 2\pi f_i$ and f_i are the eigenfrequencies of bending modes.

Following the procedure for the controller design described in the previous section, after implementing the controller, the following simulation results were obtained.
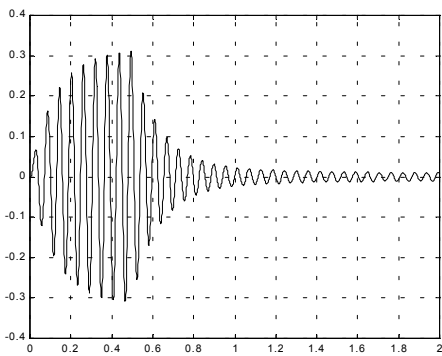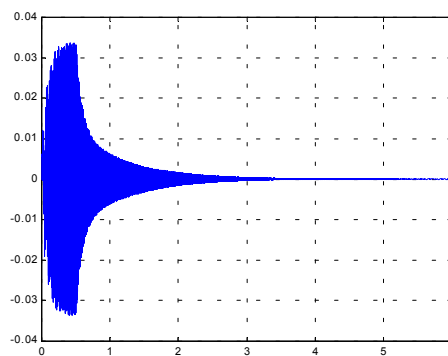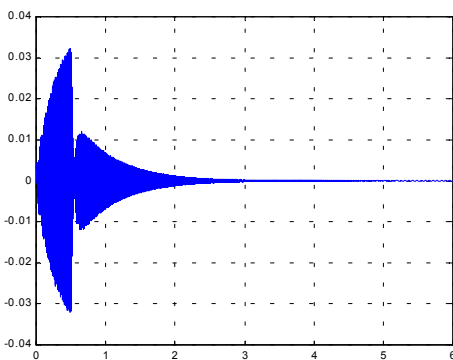

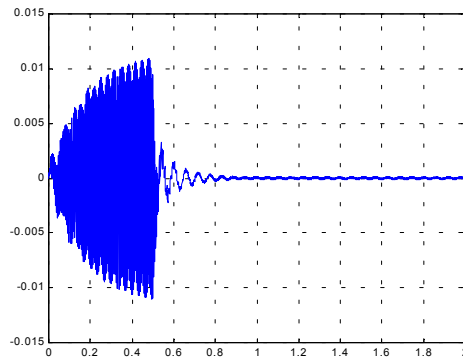
Fig. 4

Fig. 5

Fig. 6

Fig. 7

Simulation results in Fig. 4–7 were obtained for different combinations of the reference input and disturbance frequencies. For the purpose of discrete-time control system design sampling interval T=0.0001sec was chosen. Each of the diagrams represents comparison of the beam end oscillations without control and with control switched 0.5 sec after the beginning of the simulation. The vibration suppression is obvious.

Results in Fig. 4 were obtained for the case when the excitation forces have the frequency corresponding to the first bending mode eigenfrequency, i.e. F=0.01sin($2\pi\cdot17.2t$). Reference input in this case is the sine signal of the same frequency. Weighting matrices $\mathbf{Q}$ and $\mathbf{R}$ for the optimal LQ controller design were chosen in the following way: $\mathbf{Q}=10^{-7}\cdot\mathbf{I}_{10\times10}$, $\mathbf{R}=\mathbf{I}_{4\times4}$.

For the disturbance force F=0.01sin($2\pi\cdot108.6t$), corresponding to the second bending mode eigenfrequency f_2=108.6 Hz, simulation results are shown in Fig. 5. In this case in order to achieve better vibration suppression as well as the reduction of the oscillation frequency, the reference input was specified to be F=0.01sin($2\pi\cdot17.2t$). Weighting matrices were chosen in the following way: $\mathbf{Q}=10^{-5}\cdot\mathbf{I}_{10\times10}$, $\mathbf{R}=\mathbf{I}_{4\times4}$.

Fig. 6 represents results for the excitation forces F=0.01sin($2\pi\cdot302.9t$) and reference input F=0.01sin($2\pi\cdot17.2t$). Weighting matrices are: $\mathbf{Q}=10^{-2}\cdot\mathbf{I}_{10\times10}$, $\mathbf{R}=\mathbf{I}_{4\times4}$.

The result for the forces F=0.01sin($2\pi\cdot606.1t$) and reference input F=0.01sin($2\pi\cdot17.2t$) are shown in Fig. 7. Weighting matrices were chosen in the same way as in the previous case, i.e. $\mathbf{Q}=10^{-2}\cdot\mathbf{I}_{10\times10}$, $\mathbf{R}=\mathbf{I}_{4\times4}$.

In each of the tested cases the controller performed very good stability margins (upper gain margin greater than 30dB, lower gain margin less than –30dB and phase margin 128°), which means that the conroller can be considered robust from the stability margins point of view. The vibration suppression was achieved with relatively small control effort in terms of low voltage control signals, which represents a real base for the cotroller implementation.

The values of the weighting matrices $\mathbf{Q}$ and $\mathbf{R}$ affect the settling time of the closed-loop system as well as the oscillation magnitudes during the transient response. With adoped values of the weighting matrices a trade-off between the settling time and the trancient magnitudes was achieved in order to obtain satisfying results and avoid pick magnitudes at the instant when the controller is switched on. Thus presented choice of the weighting matrices represents one possible solution. Of course, with any unknown sine-excitation within the first four eigenfrequencies, the steady-state response of the closed-loop control system would be the same as in shown results for the same weighting matrices used with different excitation frequencies. Since the choice of weighting matrices affects the transient behavior after swithcing the controller on, pick magnitudes can be avoided with the controller switched on from the very beginning of the simulation. In this way the same controller can face different excitation frequencies. The simulations also showed that with appropriate choice of the reference input in combination with appropriate excitation force, tracking of desired vibration frequencies and magnitudes could also be achieved.

8. CONCLUSION

The procedure for modelling and simulation of smart structures based on a general purpose finite element software and numerical analysis of piezoelectric material systems has been presented in the paper. Discrete-time LQ optimal controller in combination with

additional dynamics tracking system has been proposed for the purpose of smart structure's vibration suppression. Applied techniques turned out to be very convenient from the simulation point of view, both in the sense of modal analysis and controller design and simulation procedure, since the proposed finite element software enables data exchange between its moduls and controller design tools like MATLAB/SIMULINK. Simulation verification of applied methods through the test-example of a clamped beam showed successful vibration suppression of the beam end in the presence of the sine-type excitation forces with frequencies corresponding to eigenfrequencies of the structure of interest. Further steps in development of this field involve ongoing experimental validations using dSpace system together with the studies of advanced test cases (like plate and shell structures) with special emphasis on the research on the possibilities of practical applications, such as vibration control of the car roof, computer tomography etc.

REFERENCES

1. Banks H. T., Smith R. C., Wang Y.: *Smart Material Structures: Modelling, Estimation and Control*, John Wiley & Sons, Chichester, Masson, Paris, 1996.
2. Berger H. Köppe H., Gabbert U., Seeger F.: *On Finite Element Analysis of Piezoelectric Controlled Smart Structures*, in Gabbert U., Tzou H. S., editors: Smart Structures and Structronic Systems, Kluwer Academic Publishers, 2001, pp. 189-196.
3. Berger H., Gabbert U., Köppe H., Seeger F.: *Finite Element Analysis and Design of Piezoelectric Controlled Smart Structures*, Journal of Theoretical and Applied Mechanics, 3, 38, 2000, pp. 475-498.
4. Clark R. L., Saunders W. R., Gibbs G. P.: *Adaptive Structures - Dynamic and Control*, J. Wiley & Sons, Inc., New York, 1998.
5. COSAR - General Purpose Finite Element Package: *Manual*, FEMCOS mbH Magdeburg (see also: http://www.femcos.de).
6. Gabbert U., editor: *Smart Mechanical Systems – Adaptronics*, Fortschr.-Ber. VDI Reihe 11, Nr. 244, Düsseldorf: VDI Verlag 1997.
7. Gabbert U., Berger H., Köppe H., Cao X.: *On Modelling and Analysis of Piezoelectric Smart Structures by the Finite Element Method*, Applied Mechanics and Engineering, Vol. 5, No. 1, 2000, pp. 127-142.
8. Gabbert U., Köppe H., Fuchs K., Seeger F.: *Modelling of Smart Composites Controlled by Thin Piezoelectric Fibers*, in Varadan, V.V., editor: Mathematics and Control in Smart Structures, SPIE Proceedings Series, Vol. 3984, 2000, pp. 2-11.
9. Gabbert U., Tzou H. S., editors: *Smart Structures and Structronic Systems*, Kluwer Academic Publishers, 2001.
10. Gabbert U., Weber Ch.-T.: *Analysis and Optimal Design of Piezoelectric Smart Structures by the Finite Element Method*, ECCM'99 European Conference on Computational Mechanics, August 31-September 3, 1999, München, Germany
11. Köppe H., Berger H., Gabbert U., Seeger F., *Finite element analysis and design of smart structures including control*, Abschlusskolloquium des Innovationskollegs Adaptive mechanische Systeme, 17.-18. Mai 2001, O-v-G Universität Magdeburg
12. Nestorović T: *On the results of investigations of the possibilities for active control of some mechanical structures*, Otto-von-Guericke-Universität Magdeburg, Preprint des Institutes für Mechanik, IFME 2001/1
13. Nestorović Trajkov T, Köppe H., Gabbert U.: *Active Vibration Control of the Beam and Plate Structure Using Optimal Tracking System Based on LQ Controller*, Proceedings of the Symposium Recent Advances in Analytical Dynamics-Control, Stability and Differential Geometry, Mathematical Institute of Serbian Academy of Science and Art, Belgrade, April 4th 2001, (to be issued)
14. Parkus H., edit.: *Electromagnetic Interactions in Elastic Solids*, Springer Verlag, Wien, New York, 1979.
15. Preumont A.: *Vibration Control of Active Structures: An Introduction*, Kluver Academic Publishers, Dordrecht, Boston, London, 1997.
16. Rao S. S., Sunar M.: *Analysis of distributed thermopiezoelectric sensors and actuators in advanced intelligent structures*, AIAA Journal, Vol. 31, No. 7, 1993, pp. 1280-1286
17. Rodellar J., Barbat A. H., Casciati F., editors: *Advances in Structural Control*, CIMNE Barcelona, 1999.

18. Tiersten H. F.: *Linear Piezoelectric Plate Vibration*, Plenum Press, New York 1969.
19. Tzou H. S., Anderson G. L.: *Intelligent Structural Systems*, Kluwer: Academic Publishers, 1993.
20. Vaccaro R. J.: *Digital Control: A State-Space Approach*, McGraw-Hill, Inc., 1995.

MODELIRANJE, UPRAVLJANJE I SIMULACIJA AKTIVNIH KONSTRUKCIJA SA PIEZOELEKTRIČNIM ELEMENTIMA PRIMENOM METODA KONAČNIH ELEMENATA I OPTIMALNOG LQ UPRAVLJANJA

Ulrich Gabbert, Tamara Nestorović Trajkov, Heinz Köppe

U radu su predstavljena neka aktuelna dostignuća u modeliranju i numeričkoj analizi sistema sa piezoelektričnim materijalima i aktivnih konstrukcija na osnovu softvera opšte namene za analizu metodom konačnih elemenata, koji ima mogućnosti za statičku i dinamičku analizu i simulaciju. Prikazano je projektovanje i simulacija upravljane aktivne strukture, pri čemu je model objekta u prostoru stanja, dobijen postupkom analize metodom konačnih elemenata, korišćen kao polazna osnova za projektovanje kontrolera. U cilju projektovanja upravljanja za prigušenje oscilacija korišćen je upravljački aparat u diskretnom domenu – optimalni LQ kontroler u kombinaciji sa sistemom praćenja. Primena pomenutih metoda verifikovana je na primeru aktivnog upravljanja oscilacijama konzole.